Possible superconducting fluctuation and pseudogap state above T_c in $CsFe_2As_2$

Huan Yang,* Jie Xing, Zengyi Du, Xiong Yang, Hai Lin, Delong Fang, Xiyu Zhu, and Hai-Hu Wen†

National Laboratory of Solid State Microstructures, Center for Superconducting Physics and Materials, School of Physics, Collaborative Innovation Center for Advanced Microstructures, Nanjing University, Nanjing 210093, China

(Received 26 April 2016; revised manuscript received 6 June 2016; published 21 June 2016)

Resistive, magnetization, torque, specific heat, and scanning tunneling microscopy measurements are carried out on heavily-hole-doped $CsFe_2As_2$ single crystals. A characteristic temperature $T^* \sim 13$ K, which is several times higher than the superconducting transition temperature $T_c = 2.11$ K, is observed and possibly related to the superconducting fluctuation or the pseudogap state. A diamagnetic signal detected by torque measurements starts from the superconducting state, remains finite, and vanishes gradually until a temperature near T^*. Temperature-dependent resistivity and specific heat also show kinks near T^*. An asymmetric gap-like feature with the energy of 8.4 meV and a symmetric superconductivity-related gap of 2.4 meV on the scanning tunneling spectra are detected, and the pseudogap-related features disappear at temperatures up to at least 9 K. These observations by different experimental tools suggest the possible existence of superconducting fluctuations or a pseudogap state in the temperature range up to four to six times T_c in $CsFe_2As_2$.

DOI: 10.1103/PhysRevB.93.224516

I. INTRODUCTION

The iron-based superconductors and cuprates are the only two unconventional systems with high-temperature superconductivity. Superconductivity can be achieved by doping electrons or holes in the parent compounds in these two systems when the antiferromagnetic order is suppressed, so these two systems have rather similar doping phase diagrams [1,2]. The pseudogap (PG) is an important feature on the phase diagram of cuprates and has attracted much experimental and theoretical attention [3]. The relationship between PG and superconductivity in cuprates is still under debate [3,4], which challenges the basic description of a Landau Fermi liquid. A recent scanning tunneling microscopy (STM) study suggests that the PG in $Bi_2Sr_2CaCu_2O_{8-\delta}$ is the intrinsic property of charge reservoir BiO layers and has very little relation to superconductivity [5]. The PG is not quite common but is also observed in several families of iron-based superconductors, based on different measurements [6–12] and even has similar doping-dependent behavior in Co-doped iron pnictides as in cuprates [10,13,14]. Superconducting fluctuation (SCF) is another important property in cuprates, which was proved by the Nernst signal and diamagnetic magnetization far above T_c [15]. In contrast, the temperature range of SCF in iron pnictides seems not so wide [16–19].

Although there is very rich physics in the two high-T_c systems, as mentioned above, the superconducting mechanism has not been settled yet. For the gap symmetry, cuprates have the well-known and dominant d-wave gap, while the situation in iron-based superconductors is very complex because Fermi-surface topologies are tremendously different in different materials [20]. A widely accepted pairing symmetry for some iron pnictides is the $s_\pm$ pairing manner which needs the nesting condition between the hole and electron pockets with almost-equal sizes [21], and this picture gets some support from STM [22,23] and other measurements. AFe_2As_2 ($A =$ K, Cs, Rb) is in the extremely-hole-doping level of the 122 family in iron pnictides. It is assumed that the correlation effect is getting more and more strong starting from the parent phase $BaFe_2As_2$ to the heavily-hole-doped case in AFe_2As_2 ($A =$ K, Cs, Rb). The pairing symmetry of these materials may be different from the early proposed $s_\pm$ since they have only the hole pockets. A nodal superconducting gap was suggested in AFe_2As_2 by different methods [24–28]. Our recent work on KFe_2As_2 reports a Van Hove singularity just several meV below the Fermi level (E_F), and it has an essential influence on superconductivity in the material [29]. The critical temperature T_c of the AFe_2As_2 family under a pressure less than 3.3 GPa shows a universal V-shaped phase diagram [30,31]. Another report shows two separate superconducting regions under high pressure up to 33 GPa in KFe_2As_2, and T_c suddenly jumps to about 11 K at 14.4 GPa in the second superconducting phase followed by a sign change of the Hall coefficient [32]. All of these indicate that the physics in the heavily-hole-doped systems AFe_2As_2 ($A =$ K, Cs, Rb) may be more complex than the lightly doped systems. This inspires us to investigate the rich physics of these systems with different experimental tools. In this paper, we report experimental results on $CsFe_2As_2$ single crystals from multiple measurements. We find a clear characteristic temperature $T^* \sim 13$ K which may correspond to the SCF or the PG state temperature and is much higher than T_c. This phenomenon adds new ingredients in understanding the correlation effect and superconductivity in these complex systems.

II. EXPERIMENTS

$CsFe_2As_2$ single crystals were synthesized by using the self-flux method [33]. The Cs chunks and Fe and As powders were weighted according to the ratio Cs : Fe : As = 6 : 1 : 6. The mixture was put into an alumina crucible which was sealed in a tantalum crucible in a high-purity argon atmosphere. The crucible sealed in an evacuated quartz tube was slowly heated up to 200 °C and held at this temperature for 6 h. It was then heated to 950 °C and held for 10 h, then cooled down to 550 °C at the rate of 3 °C/h to grow single crystals. The

*huanyang@nju.edu.cn
†hhwen@nju.edu.cn

sample was cooled down to room temperature by shutting off the power of the furnace. Shiny plate-like single crystals can be obtained from black CsAs flux. The extra flux on the surface of the crystal can be effectively washed off by deionized water or alcohol. The magnetization measurements were carried out by a superconducting quantum interference device system (SQUID-VSM; Quantum Design), while the resistance, specific heat, and torque data were measured by a physical-property measurement system PPMS-16 (Quantum Design). The scanning tunneling microscopy or spectroscopy (STM or STS) measurements were done with an ultrahigh vacuum, low temperature, and high-magnetic-field scanning probe microscope USM-1300 (Unisoku Co., Ltd.).

III. RESULTS

Figure 1(a) shows the temperature dependence of the mass magnetization (M) after zero-field-cooled (ZFC) and field-cooled (FC) processes at 10 Oe. Figure 1(b) shows temperature-dependent resistivity measured at different magnetic fields with the lowest temperature down to 1.9 K, by which one can determine the zero-resistance transition temperature $T_{c0} = 2.11$ K at 0 T. Then we use a power function $\rho(T) = \rho_0 + AT^n$ to fit the experimental resistive curve measured at 0 T from 2.4 to 10 K, and the fitting result with $\rho_0 = 1.43\ \mu\Omega$ cm and $n = 1.7$ is shown as a solid red line in Fig. 1(b). Compared with the resistivity of 590 $\mu\Omega$ cm of this sample measured at 300 K (data not shown here), we can obtain the residual-resistance ratio $r_{\mathrm{RRR}} \equiv \rho(T = 300\ \mathrm{K})/\rho_0 = 413$, which is much smaller than that reported in KFe_2As_2 [34]

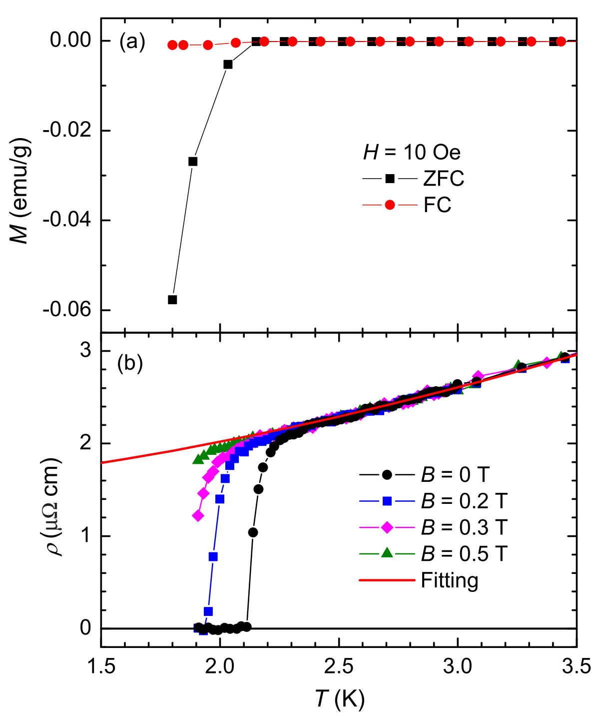

FIG. 1. (a) Temperature dependence of magnetization in $CsFe_2As_2$ after ZFC and FC processes. (b) Temperature-dependent resistivity at different magnetic fields. The red line is a power-function fit to the experimental resistive curve measured at zero field from 2.4 to 10 K.

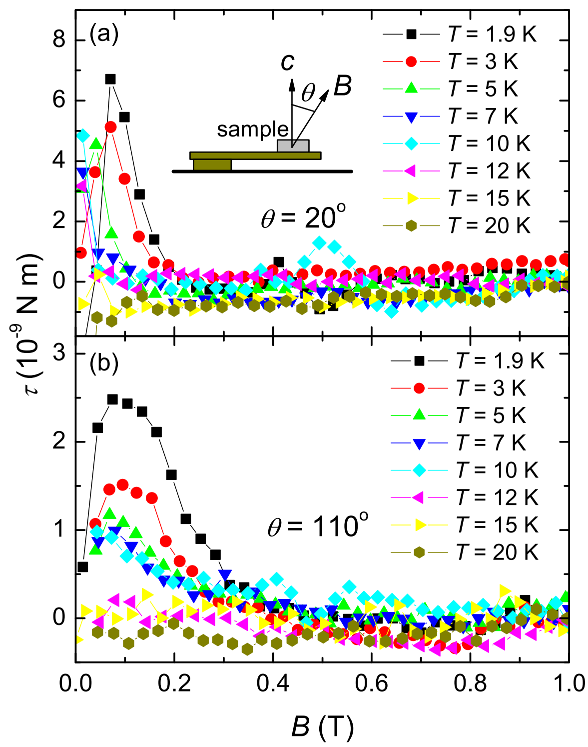

FIG. 2. Field dependence of torque signal measured at different temperatures with the angle between the magnetic field and c axis of the sample at (a) $\theta = 20^\circ$ and (b) $\theta = 110^\circ$. The inset in panel (a) shows the measurement configuration and the definition of θ.

and larger than the values in the same material from previous reports [27,35]. The zero-field resistivity curve shows a very narrow superconducting fluctuating region with the width of about 0.2 K near the onset transition temperature if we use the red fit as the normal-state resistivity. The sample is still in the zero-resistance state at 1.9 K and 0.2 T from the resistivity curve, while the superconductivity has already become very weak when the field increases to 0.5 T at the same temperature.

A diamagnetic magnetization signal above T_c measured in cuprates by torque magnetometry is shown to be an efficacious proof of the SCF beside the Nernst signal [36]. The data of magnetic-field-dependent (B-dependent) torque signal measured at different temperatures are shown in Fig. 2. The angle θ between the magnetic field and c axis of the sample [shown in the inset of Fig. 2(a)] are 20° and 110° for Figs. 2(a) and 2(b), respectively. The two selected angles correspond to the positions for maximum and minimum values in angle-dependent torque magnitude measured at 1.9 K and 0.2 T. The measured torque can be expressed as $\vec{\tau} = \vec{m} \times \vec{B}$, where $\vec{m}$ is the magnetic moment of the sample and is proportional to the magnetization. In the superconducting state, the diamagnetic magnetization should be a function of B as done in the magnetization curve with increasing B from zero field. As the product of the magnetization and the magnetic field, the torque signal should begin from zero at zero magnetic field and then reach the maximum followed by a decrease to zero when the magnetic field destroys the superconductivity. The existence of the extremum values in angle-dependent torque suggests the anisotropic magnetization

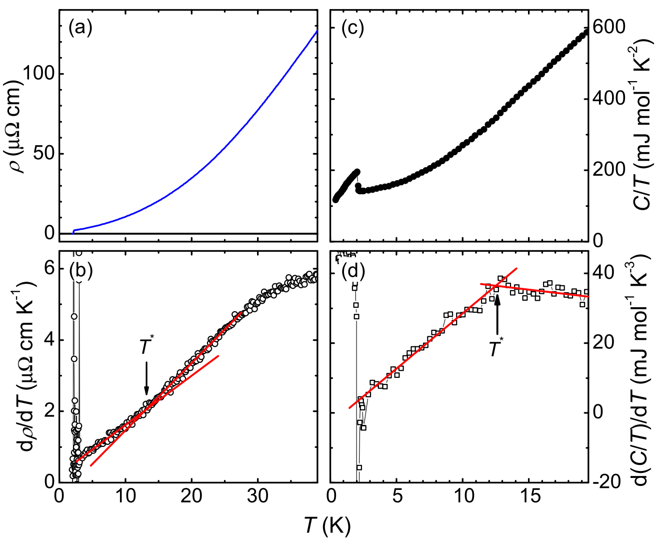

FIG. 3. Temperature dependence of (a) resistivity and (c) specific heat and the corresponding differential curves [panels (b) and (d), respectively] over a wide temperature range. One can find the kink behavior in both differential curves at about $T^* = 13$ K, as denoted by the arrows. The red solid lines are to guide the eyes.

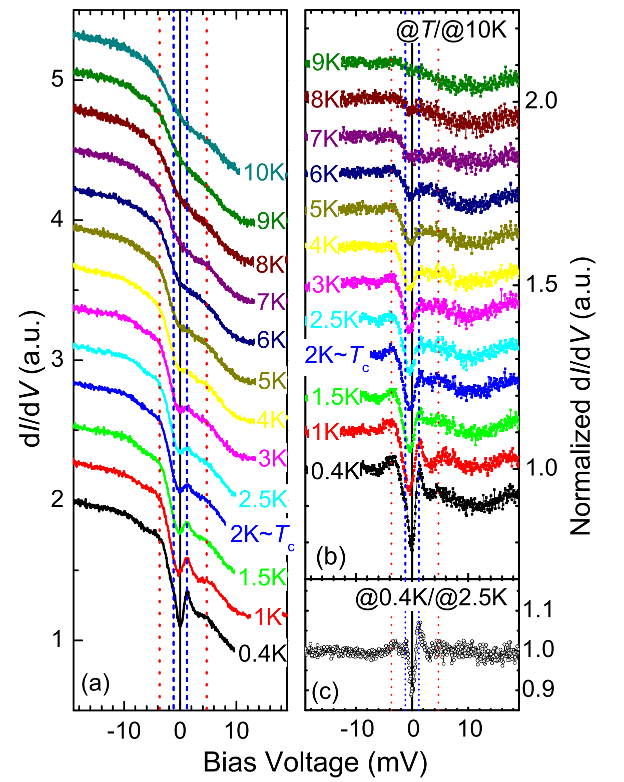

FIG. 4. (a) Evolution of STS spectra measured from 0.4 to 10 K. (b) STS spectra normalized by the STS spectrum measured at 10 K. (c) STS spectrum measured at 0.4 K normalized by the STS spectrum measured at 2.5 K just above the bulk T_c. Beside the superconducting gap peaks near ±1.2 mV, there is another pair of asymmetric gap features locating at -3.7 and 4.7 mV on the spectra.

of the sample in the superconducting state. The sample is obviously in its mixed state when $B < 0.5$ T at 1.9 K from Fig. 1(b), so the torque signal measured in the same conditions is from the superconducting diamagnetic effect. The torque-signal peak always exists and does not change its sign when the temperature is increased, crossing the critical temperature of 2.11 K, but the magnitude of the the signal reduces and finally disappears into the background above 12 K for both configurations. The sample should be very tiny for the torque measurement, and the magnetization is also weakened by increasing the magnetic field. Thus, it is difficult to judge the exact magnetic field at which the diamagnetic signal disappears. The onset field B_c^τ at which the torque signal merges to the background in Figs. 2(a) and 2(b) at 1.9 K is about 0.2 T ($\theta = 20^\circ$) or 0.4 T ($\theta = 110^\circ$) in our resolution. We can see from Fig. 2 that B_c^τ is temperature dependent and shows anisotropy for the two angles within the experimental resolution. B_c^τ shifts about 0.3 T in the temperature range from 1.9 to 7 K at $\theta = 20^\circ$, and it shifts less than 0.2 T for the same temperature range at $\theta = 110^\circ$. Here in the former situation the major component of magnetic field is along the c axis, while in the latter case, the magnetic field is almost parallel to the ab plane. The B_{c2}-T slope (dB_{c2}/dT) with magnetic field parallel to the ab plane is usually much larger than that with magnetic field along the c axis in iron pnictides. The anisotropy of dB_c^τ/dT is larger than 1.5, which is estimated from torque measurements in $CsFe_2As_2$. Although such anisotropy is not accurate because of the low signal-to-noise ratio, the anisotropy of dB_c^τ/dT agrees qualitatively with that of dB_{c2}/dT. Such anisotropy may be another proof of the torque signal from the superconducting diamagnetic effect.

We observe that a diamagnetic signal disappears above 12 K in the torque measurement; however the SCF seems not so strong from the resistive measurement near the transition, as shown in Fig. 1(b). Then we analyze the resistivity data over a wider temperature region in Fig. 3(a) and calculate the temperature derivative of the resistivity data, as shown in Fig. 3(b). One can find a kink at $T^* = 13$ K and the slope changes a bit on both sides. Heat capacity is a very sensitive method to detect bulk properties of phase transitions. The superconducting transition can be observed in the specific heat data, as shown in Fig. 3(c), which is similar to the previous report [35]. One can find an obvious turning point near $T^* = 13$ K from the temperature-dependent differential specific heat in Fig. 3(d). Therefore one can draw a self-consistent conclusion that there is a characteristic temperature at which both the resistivity and the specific heat show a kink in their temperature-derivative curves. This temperature is also near that where the torque signal disappears. We argue that this may correspond to the transition for the possible SCF, and the transition temperature is about six times T_c.

We also carried out STS measurements on the $CsFe_2As_2$ single crystals to detect the local electronic properties. A typical set of STS spectra measured at different temperatures is shown in Fig. 4. In KFe_2As_2, a Van Hove singularity was detected just a few meV below E_F, and it generates a strong DOS peak observed on the STS spectra over a wide energy range of dozens of meV[29]. However, there is no obvious peak near E_F on the spectra in $CsFe_2As_2$, which suggests that the possible Van Hove singularity is far from the Fermi energy due to the subtle change of the band structures between KFe_2As_2 and $CsFe_2As_2$. However, the spectrum in $CsFe_2As_2$ has an asymmetric background for the two sides above and below the Fermi level, which is similar to that in KFe_2As_2 and consistent with an energy-dependent density of states (DOS) of AFe_2As_2 from theoretical calculations [37]. From the spectrum measured at 0.4 K normalized by the spectrum measured at 2.5 K, as shown in Fig. 4(c), we can find a superconducting gap with a peak-peak separation of 2×1.2 meV, which is comparable with that in KFe_2As_2. However, the real superconducting-gap value depends on the detailed fitting with gap symmetry of the sample. In addition, there is also quite a high ungapped DOS on the Fermi level, which is similar to the situation in KFe_2As_2. Beside the symmetric coherence peaks of the sample, there are also two asymmetric gap features with the peak position near -3.7 and 4.7 mV, as shown by the dotted lines in Figs. 4(b) and 4(c). This asymmetric feature may be induced by the asymmetric background of the DOS on energy. It should be noted that the coherence-peak-like feature almost disappears at 2.5 K above the bulk T_c, but the asymmetric large-gap feature near E_F extends to at least 9 K. The gap feature is not observable above 10 K partially because of the thermal broadening effect. It is difficult to find such similar gapped features on KFe_2As_2 because of the strong peak near E_F from the Van Hove singularity, but we can also find some trace of the dip feature at E_F on the spectra measured just above T_c [29]. Since the bulk superconducting transition temperature is 2.11 K in $CsFe_2As_2$, as shown in Fig. 1(b), the two-gap feature above T_c may be related to the PG or SCF mentioned above.

IV. DISCUSSION

In the cuprates, the PG is regarded as a symmetric gap directly developed from the superconducting gap above T_c and with support from the bulk measurements, e.g., resistivity, nuclear magnetic resonance, specific heat, Nernst effect, etc. [3,4]. From our STS data, we find two energy gaps, i.e., one smaller gap $2\Delta_1 = 2.4$ meV which is closely related to the superconductivity with symmetric peak energies to E_F and the other $2\Delta_2 = 8.4$ meV with asymmetric peak energies with respect to E_F. Previously, the asymmetric PG-like feature was also observed above T_c on overdoped $Na(Fe_{1-x}Co_x)As$ [11], so we cannot exclude the possibility of the asymmetric gap feature as the consequence of the PG. The asymmetric PG-like features observed in both systems make the PG in the iron pnictides more interesting and need further investigation. Since there is an 80%–90% ungapped DOS near E_F and an asymmetric background of the DOS in the normal state, it is very difficult to recognize which gap is related to the possible PG in the material. Both gaps seem to disappear above T_c, and the larger-gap feature even exists up to at least 9 K. It is actually difficult to determine the ending temperature for the PG feature because of the thermal broadening effect. We have found self-consistent support from the bulk resistance and specific heat measurement from which a characteristic temperature $T^* \sim 13$ K is observed. Here, with the two possible PG values, one can obtain the reduced gap ratios $2\Delta_1/k_B T_c = 11.6$ and $2\Delta_2/k_B T_c = 45$ which are both in the range 9–46 summarized in the "1111-family" iron-based superconductors [38].

One of the early understandings for the PG in cuprates was its close relationship to Cooper pairing above T_c; however, critical temperatures for SCF and PG states were divorced from each other by a careful STS measurement [39]. The PG in the normal state is also regarded as a consequence of phase-incoherent Cooper pairs in iron-based superconductors [17]. Recently, it was concluded that SCF may be very strong in the FeSe single crystals because of the vicinity to the BEC-BCS crossover [40]. This recommends a picture of preformed Cooper pairs with phase incoherence. In our experiments, the diamagnetic signal was detected by torque measurements up to more than 12 K, and the critical field B_c^τ above T_c has a temperature dependence as well as an anisotropy to the angle between the magnetic field and c axis of the crystal. The characteristic temperature derived from different experimental tools (beside that from resistivity) is also near $T^* \sim 6T_c$. Since the excess conductivity due to the possible SCF is not observed, we thus cannot conclude that the PG effect is due to the SCF. As addressed in early transport measurements by resistivity and Nernst in cuprates, the resistivity is less pronounced to illustrate the SCF compared with the Nernst signal. Therefore, a Nernst measurement is highly desired although the temperature is very low and the window is quite narrow. However, either the PG feature or SCF in present system should be closely connected to the complex and usual normal-state properties in $CsFe_2As_2$.

V. CONCLUDING REMARKS

By using torque measurements, we observed the diamagnetic signal at temperatures 6 times T_c in $CsFe_2As_2$ single crystals. This is explained by the possible superconducting fluctuation effect. Supporting evidence is obtained by analyzing the derivative of resistivity and specific heat, both of which illustrate a characteristic temperature $T^* \sim 13$ K. In addition, the pseudogap feature is detected as the appearance of two sets of energy gaps existing above T_c on the tunneling spectra. All these facts point to a picture that there is a pseudogap effect in $CsFe_2As_2$. Our results provide extra information for unraveling the usual normal state and also the superconducting mechanism in iron-based superconductors.

ACKNOWLEDGMENTS

This work is supported by the NSF of China, the Ministry of Science and Technology of China (973 Projects No. 2011CBA00102 and No. 2012CB821403).

[1] D. N. Basov and A. V. Chubukov, Nat. Phys. **7**, 272 (2011).
[2] H. H. Wen and S. L. Li, Annu. Rev. Condens. Matter Phys. **2**, 121 (2011).
[3] Kordyuk, Low Temp. Phys. **41**, 319 (2015).
[4] T. Timusk and B. W. Statt, Rep. Prog. Phys. **62**, 61 (1999).

[5] Y. F. Lv, W. L. Wang, J. P. Peng, H. Ding, Y. Wang, L. L. Wang, K. He, S. H. Ji, R. D. Zhong, J. Schneeloch, G. D. Gu, C. L. Song, X. C. Ma, and Q. K. Xue, Phys. Rev. Lett. **115**, 237002 (2015).
[6] C. Hess, A. Kondrat, A. Narduzzo, J. E. Hamann-Borrero, R. Klingeler, J. Werner, G. Behr, and B. Buchner, Europhys. Lett. **87**, 17005 (2009).
[7] T. Mertelj, V. V. Kabanov, C. Gadermaier, N. D. Zhigadlo, S. Katrych, J. Karpinski, and D. Mihailovic, Phys. Rev. Lett. **102**, 117002 (2009).
[8] Y.-M. Xu, P. Richard, K. Nakayama, T. Kawahara, Y. Sekiba, T. Qian, M. Neupane, S. Souma, T. Sato, T. Takahashi, H.-Q. Luo, H.-H. Wen, G.-F. Chen, N.-L. Wang, Z. Wang, Z. Fang, X. Dai, and H. Ding, Nat. Commun. **2**, 392 (2011).
[9] Y. M. Dai, B. Xu, B. Shen, H. H. Wen, J. P. Hu, X. G. Qiu, and R. P. S. M. Lobo, Phys. Rev. B **86**, 100501(R) (2012).
[10] M. A. Tanatar, N. Ni, A. Thaler, S. L. Bud'ko, P. C. Canfield, and R. Prozorov, Phys. Rev. B **82**, 134528 (2010).
[11] X. D. Zhou, P. Cai, A. F. Wang, W. Ruan, C. Ye, X. H. Chen, Y. Z. You, Z. Y. Weng, and Y. Y. Wang, Phys. Rev. Lett. **109**, 037002 (2012).
[12] S. J. Moon, A. A. Schafgans, S. Kasahara, T. Shibauchi, T. Terashima, Y. Matsuda, M. A. Tanatar, R. Prozorov, A. Thaler, P. C. Canfield, A. S. Sefat, D. Mandrus, and D. N. Basov, Phys. Rev. Lett. **109**, 027006 (2012).
[13] S. H. Baek, H. J. Grafe, L. Harnagea, S. Singh, S. Wurmehl, and B. Büchner, Phys. Rev. B **84**, 094510 (2011).
[14] M. Matusiak and T. Wolf, Phys. Rev. B **92**, 020507(R) (2015).
[15] Y. Wang, L. Li, and N. P. Ong, Phys. Rev. B **73**, 024510 (2006).
[16] Z. W. Zhu, Z. A. Xu, X. Lin, G. H. Cao, C. M. Feng, G. F. Chen, Z. Li, J. L. Luo, and N. L. Wang, New J. Phys. **10**, 063021 (2008).
[17] G. Sheet, M. Mehta, D. A. Dikin, S. Lee, C. W. Bark, J. Jiang, J. D. Weiss, E. E. Hellstrom, M. S. Rzchowski, C. B. Eom, and V. Chandrasekhar, Phys. Rev. Lett. **105**, 167003 (2010).
[18] A. Pourret, L. Malone, A. B. Antunes, C. S. Yadav, P. L. Paulose, B. Fauqué, and K. Behnia, Phys. Rev. B **83**, 020504(R) (2011).
[19] A. Ramos-Álvarez, J. Mosqueira, F. Vidal, D. Hu, G. F. Chen, H. Q. Luo, and S. L. Li, Phys. Rev. B **92**, 094508 (2015).
[20] J. P. Hu and J. Yuan, Front. Phys. **11**, 117404 (2016).
[21] I. I. Mazin, D. J. Singh, M. D. Johannes, and M. H. Du, Phys. Rev. Lett. **101**, 057003 (2008).
[22] T. Hanaguri, S. Niitaka, K. Kuroki, and H. Takagi, Science **328**, 474 (2010).
[23] H. Yang, Z. Y. Wang, D. L. Fang, Q. Deng, Q.-H. Wang, Y.-Y. Xiang, Y. Yang, and H.-H. Wen, Nat. Commun. **4**, 2749 (2013).
[24] K. Hashimoto, A. Serafin, S. Tonegawa, R. Katsumata, R. Okazaki, T. Saito, H. Fukazawa, Y. Kohori, K. Kihou, C. H. Lee, A. Iyo, H. Eisaki, H. Ikeda, Y. Matsuda, A. Carrington, and T. Shibauchi, Phys. Rev. B **82**, 014526 (2010).
[25] K. Okazaki, Y. Ota, Y. Kotani, W. Malaeb, Y. Ishida, T. Shimojima, T. Kiss, S. Watanabe, C. T. Chen, K. Kihou, C. H. Lee, A. Iyo, H. Eisaki, T. Saito, H. Fukazawa, Y. Kohori, K. Hashimoto, T. Shibauchi, Y. Matsuda, H. Ikeda, H. Miyahara, R. Arita, A. Chainani, and S. Shin, Science **337**, 1314 (2012).
[26] J. P. Reid, M. A. Tanatar, A. Juneau-Fecteau, R. T. Gordon, S. R. de Cotret, N. Doiron-Leyraud, T. Saito, H. Fukazawa, Y. Kohori, K. Kihou, C. H. Lee, A. Iyo, H. Eisaki, R. Prozorov, and L. Taillefer, Phys. Rev. Lett. **109**, 087001 (2012).
[27] X. C. Hong, X. L. Li, B. Y. Pan, L. P. He, A. F. Wang, X. G. Luo, X. H. Chen, and S. Y. Li, Phys. Rev. B **87**, 144502 (2013).
[28] Z. Zhang, A. F. Wang, X. C. Hong, J. Zhang, B. Y. Pan, J. Pan, Y. Xu, X. G. Luo, X. H. Chen, and S. Y. Li, Phys. Rev. B **91**, 024502 (2015).
[29] D. L. Fang, X. Shi, Z. Y. Du, P. Richard, H. Yang, X. X. Wu, P. Zhang, T. Qian, X. X. Ding, Z. Y. Wang, T. K. Kim, M. Hoesch, A. F. Wang, X. H. Chen, J. P. Hu, H. Ding, and H. H. Wen, Phys. Rev. B **92**, 144513 (2015).
[30] F. F. Tafti, A. Juneau-Fecteau, M. È. Delage, S. René de Cotret, J. P. Reid, A. F. Wang, X. G. Luo, X. H. Chen, N. Doiron-Leyraud, and L. Taillefer, Nat. Phys. **9**, 349 (2013).
[31] F. F. Tafti, A. Ouellet, A. Juneau-Fecteau, S. Faucher, M. Lapointe-Major, N. Doiron-Leyraud, A. F. Wang, X. G. Luo, X. H. Chen, and L. Taillefer, Phys. Rev. B **91**, 054511 (2015).
[32] Y. Nakajima, R. X. Wang, T. Metz, X. F. Wang, L. M. Wang, H. Cynn, S. T. Weir, J. R. Jeffries, and J. Paglione, Phys. Rev. B **91**, 060508(R) (2015).
[33] K. Kihou, T. Saito, S. Ishida, M. Nakajima, Y. Tomioka, H. Fukazawa, Y. Kohori, T. Ito, S. Uchida, A. Iyo, C. H. Lee, and H. Eisaki, J. Phys. Soc. Jpn. **79**, 124713 (2010).
[34] A. F. Wang, S. Y. Zhou, X. G. Luo, X. C. Hong, Y. J. Yan, J. J. Ying, P. Cheng, G. J. Ye, Z. J. Xiang, S. Y. Li, and X. H. Chen, Phys. Rev. B **89**, 064510 (2014).
[35] A. F. Wang, B. Y. Pan, X. G. Luo, F. Chen, Y. J. Yan, J. J. Ying, G. J. Ye, P. Cheng, X. C. Hong, S. Y. Li, and X. H. Chen, Phys. Rev. B **87**, 214509 (2013).
[36] Y. Y. Wang, L. Li, M. J. Naughton, G. D. Gu, S. Uchida, and N. P. Ong, Phys. Rev. Lett. **95**, 247002 (2005).
[37] Y. Mizukami, Y. Kawamoto, Y. Shimoyama, S. Kurata, H. Ikeda, T. Wolf, D. A. Zocco, K. Grube, H. v. Löhneysen, Y. Matsuda, and T. Shibauchi, arXiv:1510.02273.
[38] H. W. Ou, Y. Zhang, J. F. Zhao, J. Wei, D. W. Shen, B. Zhou, L. X. Yang, F. Chen, M. Xu, C. He, R. H. Liu, M. Arita, K. Shimada, H. Namatame, M. Taniguchi, Y. Chen, X. H. Chen, and D. L. Feng, Solid State Commun. **148**, 504 (2008).
[39] T. Kondo, Y. Hamaya, A. D. Palczewski, T. Takeuchi, J. S. Wen, Z. J. Xu, G. D. Gu, J. Schmalian, and A. Kaminski, Nat. Phys. **7**, 21 (2011).
[40] S. Kasaharaa, T. Watashigea, T. Hanagurib, Y. Kohsakab, T. Yamashitaa, Y. Shimoyamaa, Y. Mizukamia, R. Endoa, H. Ikedaa, K. Aoyamaa, T. Terashimae, S. Ujie, T. Wolff, H. von Löhneysenf, T. Shibauchia, and Y. Matsuda, Proc. Natl. Acad. Sci. USA **111**, 16309 (2014).